

In-situ TEM study of the crystallization of $\text{Ge}_2\text{Sb}_2\text{Te}_5$

B.J. Kooi*, W.M.G. Groot, J.Th.M. De Hosson

Department of Applied Physics, Materials Science Centre and Netherlands Institute for Metals Research, University of Groningen, Nijenborgh 4, 9747 AG Groningen, The Netherlands

Abstract

Crystallization of amorphous $\text{Ge}_2\text{Sb}_2\text{Te}_5$ films (10, 40 and 70 nm thick) was studied by in-situ heating in a transmission electron microscope (TEM). Electron irradiation induced crystallization is possible at room temperature using a 400 kV electron beam where the reciprocal of the incubation time for crystallization scales linearly with the current density during electron irradiation. Without electron-beam exposure, crystallization starts at 130 °C. Using a 200 kV beam, crystallization also occurred in the temperature interval between 70 and 130 °C. In principle electron irradiation always affects the crystallization kinetics, promoting nucleation and probably hindering growth. At 130 °C without electron-beam exposure, 400 nm diameter colonies of 10-20 nm grains develop in the 40 and 70 nm thick films showing clear symmetric bending contour contrast. These spherulites prefer to have in their center the $\langle 111 \rangle$ zone axis of the $\text{Fm}\bar{3}m$ structure perpendicular to the film surface and show a typical tilt variation of $\pm 10^\circ$. At 340 °C the transition from the meta-stable to the stable trigonal ($\text{P}\bar{3}m1$) crystal structure takes place. Fast and excessive grain growth occurs with the [0001] axis perpendicular to the film surface. (Partial) oxidation of the $\text{Ge}_2\text{Sb}_2\text{Te}_5$ film reduced the crystallization temperature from 130 to 35 °C.

Introduction

In phase change optical recording, $\text{Ge}_2\text{Sb}_2\text{Te}_5$ is currently most widely used as the active medium for rewriteable information storage [1-4]. Amorphous areas embedded in a crystalline surrounding act as bits of information. A relatively high laser power is used to write these amorphous spots and medium and low laser powers are used for erasing (recrystallization) and reading, respectively.

This paper focuses on the crystallization of 10, 40 and 70 nm thick amorphous $\text{Ge}_2\text{Sb}_2\text{Te}_5$ films studied using in-situ annealing in a TEM. Particularly the influence of the electron beam of the TEM on the kinetics and morphology of crystallization is addressed. Also a strong influence of oxidation of $\text{Ge}_2\text{Sb}_2\text{Te}_5$ on the crystallization temperature is detected.

Experimental

Homogeneous $\text{Ge}_2\text{Sb}_2\text{Te}_5$ master alloys were produced by mixing the pure components (Ge:6N, Sb and Te both 5N) in an evacuated quartz tube at 750 °C. Pieces of the ingot were positioned in pockets for electron beam evaporation. As substrates 10 nm thick Si-nitride membranes were used. These transparent substrates were obtained by etching 100 x 100 μm^2 windows in a Si wafer containing the thin Si-nitride film on one side. A Varian electron beam evaporator with thickness monitor was used for the deposition of 10, 40 and 70 nm thick amorphous $\text{Ge}_2\text{Sb}_2\text{Te}_5$ films. Specimens were stored in vacuum to prevent oxidation of the $\text{Ge}_2\text{Sb}_2\text{Te}_5$ film.

For TEM a JEOL 2010F operating at 200 kV was used. A Gatan double tilt heating holder (model 652 with a model 901 SmartSet Hot Stage Controller) was used that employs a PID controller for accurately controlling of the temperature (within ± 1 °C) and for a fast ramp rate to attain the desired final temperature without overshoot. Note that the temperature of the thin area that is imaged using TEM is generally lower than the indicated nominal temperature of the heating element within

* E-mail: B.J.Kooi@phys.rug.nl

the specimen holder; the higher the temperature, the larger the discrepancy. Because the electron beam of the TEM can influence the crystallization process, we either imaged the sample at elevated temperature, but in areas that were not previously exposed to electrons, or we cooled down and imaged at room temperature (after which we continued with heating). Apart from the in-situ heating experiments in the JEOL 2010F also some experiments were performed at room temperature with a JEOL 4000EX/II TEM operating at 400 kV.

Results

Crystallization of amorphous $\text{Ge}_2\text{Sb}_2\text{Te}_5$ films at room temperature using a 400 kV electron beam of a TEM (having a probe current of 30 nA) turned out to be possible. Variation of the size of the illuminated (irradiated) area of the specimen allowed the measurement of the incubation time for crystallization (of a 40 nm thick film) as a function of current density of the electron beam. The result is presented in Fig.1. When the current density I (in $\text{nA}/\mu\text{m}^2$) is plotted versus the reciprocal of the incubation time t_i (in s^{-1}), the results can be fitted quite well by the following equation:

$$I = (3.94 \pm 0.16) 10^4 \frac{1}{t_i} + (0.17 \pm 4.8)$$

According to our expectation an infinite high current density is needed for $t_i=0$. However, a-priori we did not expect that for a current density going to zero the incubation time would go to infinity. Therefore we did not force the fit to go through $I=0$ for $1/t_i = 0$, but the resulting value $I=0.17 \pm 4.8$ shows that it effectively holds. This finding is important, because it indicates that there is no finite current density below which the incubation time goes to infinity. Thus even for the lowest dose, an effect of the electron beam on the crystallization process is expected. One can argue that if the incubation time is long enough (e.g. more than 10 hours), the effect of the corresponding electron beam on the crystallization process will be negligibly small (because at higher temperatures the kinetics is such that crystallization occurs within minutes). However, this reasoning is incorrect as we will show below.

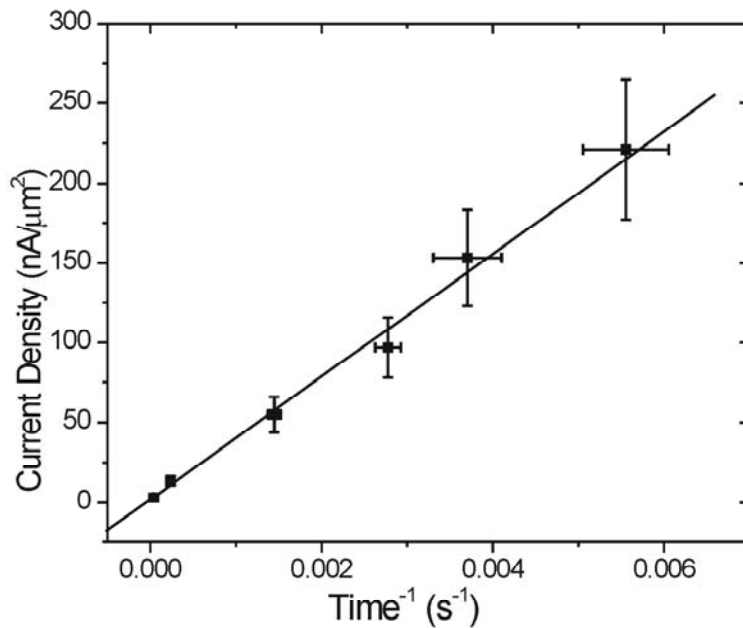


Fig.1 The reciprocal of the incubation time for crystallization of a 40 nm thick $\text{Ge}_2\text{Sb}_2\text{Te}_5$ film as a function of the current density of a 400 kV electron beam going through the film (with the sample holder at room temperature) shows that they can be linearly related.

With the sample holder at room temperature we did not observe crystallization under a 200 keV beam (having a probe current of 3 nA). However, in the temperature window between 70 and 125 °C crystallization of amorphous $\text{Ge}_2\text{Sb}_2\text{Te}_5$ was only observed when assisted by this 200 keV. Crystallization was observed after 5 min. at 80 °C when the irradiated area had a diameter of about 100 nm, at 90 °C when the beam was 400 nm wide and at 120 °C when the beam had a diameter of

1.8 μm . The results of these last 2 conditions are visible in Fig.2. At 50 $^{\circ}\text{C}$ crystallization was not observed even with the beam focused in an area with a diameter of 20 nm. At 130 $^{\circ}\text{C}$ crystallization also occurs outside the area irradiated by the electrons as can be seen in Fig.3.

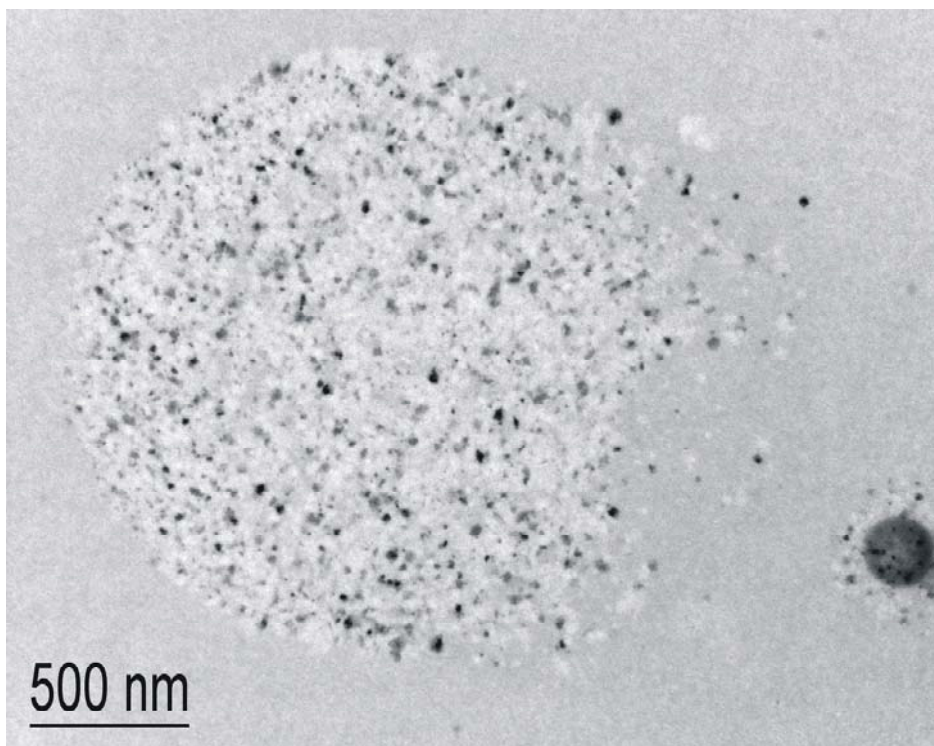


Fig.2 Bright-field TEM image showing electron-beam assisted crystallization of a 40 nm thick $\text{Ge}_2\text{Sb}_2\text{Te}_5$ film after 5 min. at 90 $^{\circ}\text{C}$ with an electron beam diameter of 400 nm (small area on the lower right) and after 5 min at 120 $^{\circ}\text{C}$ with an electron beam diameter of 1.8 μm .

Note the large difference in morphology and what at first sight appears as grain size of the crystals that were formed at 130 $^{\circ}\text{C}$ with and without electron irradiation. In the irradiated area the typical grain size is 10-20 nm and the grains have random orientations (as can be seen from SAED patterns). Outside this area apparent large grains with a typical size of 400 nm are present. Closer inspection of these large grains reveals that they are in fact colonies consisting of grains with a size of around 10 nm that have experienced cooperative growth. Most colonies show a symmetric pattern of black lines very similar to bend contours. Colonies with a 3-fold symmetry (each 60 $^{\circ}$ a black line emerges from the center) are most abundant. These symmetries reveal the strong texture that is present within the colonies. If all grains within a colony would have identical orientation (i.e. as in a single crystal) then the contrast would be more or less uniform over a colony. Here it is not. Tilting with only a few degrees shows that the symmetric black lines move across the colony like bending contours do. Because the Si-nitride substrate is flat this indicates that the grains in the center of the bend contour are exactly in a zone axis, but when moving to the periphery of the colony the grains start to tilt the zone axis in the radial direction. We observed that a tilt of typical 10 degrees is present between the center and the edge of the colony having a typical size of 400 nm. This was checked by tilting in such a way that the center of the bend contour (present in the middle of a colony) was moved to the edge of the colony. On average, the larger the diameter of the observed colony in plan view the larger the variation in tilt angle across the colony. The colonies thus strongly resemble spherulites [5]. However, note that the colony diameter is on average 400 nm compared to a thickness of 40 nm. Knowing on which side in the microscope the film/vacuum and the film/Si-nitride interface is present and observing to which (calibrated) side the center of the bend contour moves upon positive and negative tilt allows the distinction at which interface the spherulite nucleated. The results of these tilting experiments clearly demonstrate that nucleation occurs at the film/vacuum interface and not at the film/Si-nitride interface.

Spherulites were also observed in the 70 nm thick film where they tend to be slightly larger, but not in the 10 nm thick film. Apparently but not surprisingly a minimum film thickness is needed to enable the growth of the spherulites.

In Fig.3 we see that a 200 kV beam with a diameter of 5.4 μm clearly altered the kinetics and morphology of crystallization. The current density in this case was only 0.12 $\text{nA}/\mu\text{m}^2$. If we insert this value in the above equation the incubation time would be about 100 hrs at room temperature for a 400 kV electron beam and even longer for a 200 kV one. Still the effect in

Fig.3 is substantial. Hence, the conclusion is that it appears impossible to avoid the influence of the electron beam on the crystallization of $\text{Ge}_2\text{Sb}_2\text{Te}_5$.

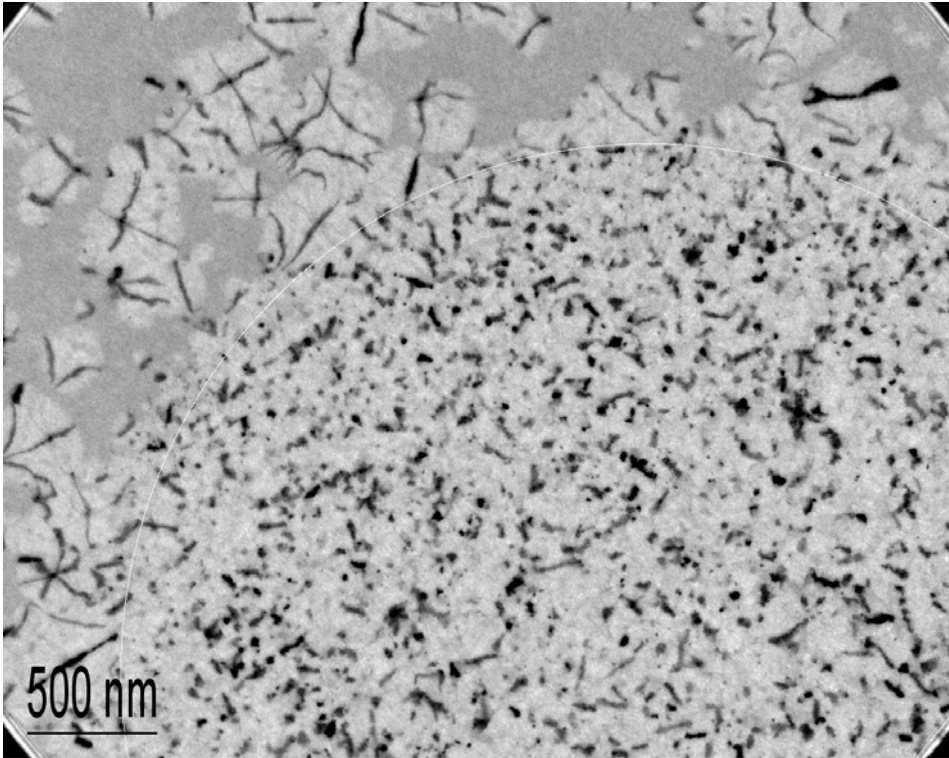


Fig.3 Bright-field TEM image showing crystallization of a 40 nm thick $\text{Ge}_2\text{Sb}_2\text{Te}_5$ film after 5 min at 130 °C both *without* (top and left side) and *with* electron-beam assistance (lower right side). Note that only a part of the electron-irradiated area with a diameter of 5.4 μm is shown and that the crystallization (both morphology and kinetics) is clearly different with and without electron-beam assistance.

After 5 min. at 130 °C crystallization inside the irradiated area is completed. However, outside this area the crystallization is finalized when the temperature is raised up to 140 °C (see Fig.4a). Fig.4b shows an SAED pattern of the area indicated by the black circle in Fig.4a. The SAED pattern matches perfectly with an fcc crystal viewed along its $\langle 111 \rangle$ zone axis having a lattice constant of 0.60 ± 0.01 nm. This pattern corresponds well with the meta-stable NaCl-type structure of $\text{Ge}_2\text{Sb}_2\text{Te}_5$ having a lattice constant of 0.601 nm [6,7]. The diffraction pattern in Fig.4b gives the impression that it originates from a single-crystal. However as explained above this is not in accordance with the bend-contour contrast present in the colonies and with the tilting experiments. The positions of the spots in the pattern in Fig.4b are not sensitive to tilt but the intensities of the spots are sensitive. If however, the tilt occurs in a radial direction symmetric around the center of the bend contour and the center of this contour is more or less in the center of the SA aperture, then the spot pattern still will have the appearance of a single crystal viewed perfectly along its zone axis.

Increasing the temperature above 140 °C does not lead to drastic changes, but increases the size of the individual crystallites in the colonies to typical 40-50 nm and results in void formation. The connected structure within the individual colonies is lost gradually during this anneal from 140 to 335 °C. Void formation has two origins: (1) Crystallization results in a denser structure due to removal of free volume from the amorphous structure. This effect is expected to be small because in the meta-stable NaCl-type crystal structure still 20 % of vacancies are present on one of the two fcc sublattices over which Ge and Sb are distributed (with Te occupying fully the other fcc sublattice). Nevertheless, a volume reduction of 6% has been reported when the meta-stable crystalline structure forms out of the amorphous one [8]. (2) Evaporation of the $\text{Ge}_2\text{Sb}_2\text{Te}_5$ film at the elevated temperatures. The images were recorded for films without a capping layer that are of course prone to evaporation in the vacuum of the TEM.

Increasing the temperature to 340 °C results in a dramatic change. Excessive grain growth occurs where the grain boundary moves fast (of the order of a second) over many micrometers. Fig.5a shows a BF-TEM image with the corresponding SAED pattern in Fig.5b. Careful inspection of Fig.5b shows that additional spots have appeared, as indicated by the arrows, compared to the $\langle 111 \rangle$ fcc zone axis pattern of Fig.4b. The pattern in 5b points at a hexagonal crystal structure viewed along its [0001] zone axis having a lattice constant $a=0.424 \pm 0.007$ nm. This lattice constant corresponds well with the stable

high temperature crystal structure of $\text{Ge}_2\text{Sb}_2\text{Te}_5$ having a and c lattice constants of 0.425 nm and 1.727 nm, respectively [9]. Note the voids with a triangular shape due to $\{11\bar{2}0\}$ facets (if these facets are observed edge-on) that were re-arranged very fast during the phase transformation. All grains orient their $[0001]$ perpendicular to the surface. Apparently the basal planes in the trigonal structure want to be parallel to the surface or to the interface with the Si-nitride (the grains have large aspect ratio and the influence of the grain-boundary energy is therefore negligibly small). Because each basal plane is only occupied by the atoms of one element, there may be a strong preference for a certain element at the surface in order to attain the lowest surface energy. It is known that thin films of amorphous Sb and Sb-Ge (with Sb > 85 at.%) after crystallization develop a strong fiber texture with $[0001]$ perpendicular to the surface [10]. Moreover, Sb is well known for its segregation tendency in many systems and for its behavior as a surfactant [11]. Therefore it is quite likely that in the present system Sb prefers to be the outermost atomic layer.

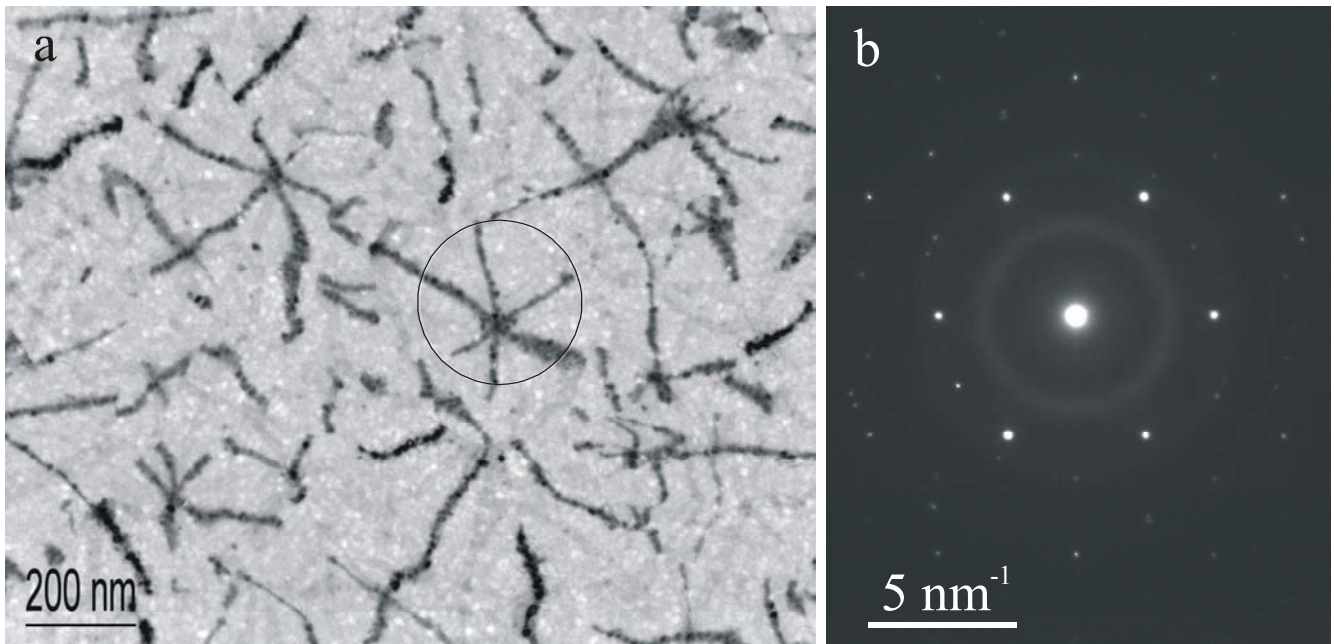


Fig.4 a. Bright-field TEM image showing a fully crystallized 40 nm thick $\text{Ge}_2\text{Sb}_2\text{Te}_5$ film after 5 min at 140 °C (without electron-beam assistance) showing crystals with bending contour contrast. **b.** Selected Area Electron Diffraction pattern of the circular area indicated in Fig.4a showing a $\langle 111 \rangle$ zone-axis pattern of an fcc material having a lattice constant of 0.60 ± 0.01 nm.

Oxidation of $\text{Ge}_2\text{Sb}_2\text{Te}_5$ has a tremendous effect on the amorphous to crystalline transition temperature (T_c). After keeping a 10 nm thick $\text{Ge}_2\text{Sb}_2\text{Te}_5$ film for 2 weeks in air (in a conditioned room) heating was hardly necessary to crystallize the whole film; a temperature of 35 °C was sufficient as can be seen in Fig.6. Notwithstanding the low temperature, crystallization occurred very fast (matter of seconds for complete crystallization). Fig.6a shows an overview BF image and Fig.6b a HRTEM image. The crystallites have a typical size of 40-50 nm and are strongly faceted. This is a totally different crystal morphology than the one observed after the normal crystallization at 130 °C (cf. Fig.3). Grain boundaries give a distinct contrast; darker than the weakly diffracting crystalline grains and brighter than the grains showing a strong diffraction contrast (cf. Fig.6a). These grain boundaries still have an amorphous structure, probably due to the presence of amorphous Ge-oxide. From the three elements present in the film, Ge has the highest oxygen affinity and is thus preferentially oxidized. The remaining film will thus become enriched in Sb and Te. It is known that the T_c decreases as the relative amount of Sb_2Te_3 increases in the pseudo-binary $\text{GeTe-Sb}_2\text{Te}_3$ system; e.g for GeTe a T_c of 170 °C is given [12], for $\text{Ge}_2\text{Sb}_2\text{Te}_5$ ~140 °C [13,14] and for $\text{Ge}_1\text{Sb}_4\text{Te}_7$ ~120 °C [13,14]. Interesting in this context is that for $\text{Ge}_x\text{Te}_{1-x}$ for x going from 0.2 to 0 the T_c decreases from about 200 to 0 °C [12]. Calculated values for the glass-transition temperature (T_g) for (all possible compositions in) the ternary Ge-Sb-Te system [14] show indeed that from $\text{Ge}_2\text{Sb}_2\text{Te}_5$ to ‘ Sb_2Te_5 ’ a decrease from 110 °C to about -10 °C occurs. Noting that the T_c is always slightly higher than T_g , the present finding fits well within this picture by a decrease from 130 to 35 °C.

Discussion

Crystallization (with the sample holder at room temperature) of amorphous $\text{Ge}_2\text{Sb}_2\text{Te}_5$ under the electron beam of a TEM was mentioned in [15]. Working at 200 kV acceleration voltage instead of the normal 400 kV (and defocusing the beam on the specimen) removed their problems with crystallization of 80 nm thick $\text{Ge}_2\text{Sb}_2\text{Te}_5$. These observations agree fully with the ones of the present work. With the TEM sample holder at room temperature crystallization is possible at 400 kV but not at 200 kV. However, with the 200 keV beam at 70 °C we could invoke crystallization after 5-10 min. under the electron beam for all 3 film thickness' investigated (10, 40 and 70 nm). Most likely, crystallization is possible at lower temperatures, but then a longer incubation time holds for crystallization. The conclusion of the present work is that even for low current densities a 200 keV beam influences the nucleation rate in $\text{Ge}_2\text{Sb}_2\text{Te}_5$ (cf. Fig.3). Still, defocusing even more strongly the beam using very small current densities may be used to minimize (although not totally avoiding) the influence of the electron beam on the crystallization process. Then the question is if the signal to noise ratio still allows fast capturing (e.g. on video tape) of images during crystallization that are clearly interpretable. Therefore, based on the present discussion it is quite remarkable that the kinetic study performed in [16] by in-situ TEM using a JEOL 4000 EX operating at 400 kV and capturing images with 25 frames/s did not suffer from influence of the electron beam on the crystallization process.

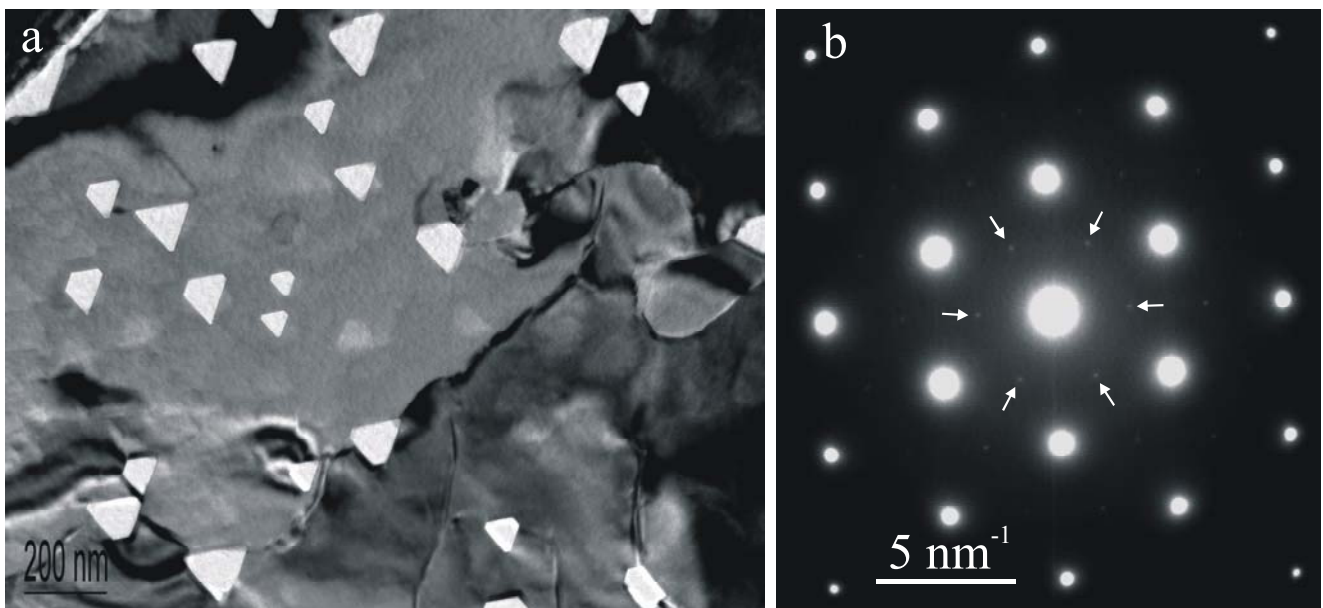


Fig.5 a. Bright-field TEM image showing the excessive grain growth that occurs at 340 °C when the meta-stable crystal structure transforms into the stable one. Voids with triangular shape develop in a single grain. **b.** SAED pattern showing perpendicular to the surface an [0001] orientation of the $\text{Ge}_2\text{Sb}_2\text{Te}_5$ crystal, with $a=0.424\pm 0.007$ nm that points at the (P 3 m1) stable crystal structure. Arrows indicate the (weak) $\{101\ 0\}$ reflections making the distinction between the stable and the meta-stable crystal structure (cf. Fig.4b).

Generally, a higher accelerating voltage reduces specimen heating and radiolysis by the electron beam, but increases displacement damage by knock-on collisions [17]. The present results and the ones reported in Ref.15 show that crystallization is more promoted at 400 kV than at 200 kV. This clearly indicates that the effect of the electron beam is displacement damage and not radiolysis or specimen heating. Also the difference in crystallization morphology inside and outside the area irradiated (cf. Fig.3) indicates that the influence of the electron beam is not a simple heating effect. Then the same morphology as observed at 130 °C would have been observed at lower temperatures under the electron beam, which is not the case.

The large colonies outside the electron-irradiated area (cf. Fig.3) indicate that nucleation is the rate-limiting step and that once a stable nucleus is formed colonies can grow relatively fast. In contrast, small randomly oriented grains are present inside the irradiated area. From this it is particularly clear that the excitations by the energetic electrons facilitate the formation of stable nuclei. Because so many nuclei are initially formed simultaneously their growth is spatially limited due

to the neighboring nuclei. A second possibility is that the growth of the crystallites is hampered by the electron irradiation and in this way the nuclei are formed sequentially over a larger time span, but that it still results in a crystallized film with only small randomly oriented grains. The observations suggest that the small crystallites are formed sequentially. This would indicate that the electron beam hampers the growth of the crystallites. A definite conclusion is that the energetic electrons promote the formation of stable crystal nuclei.

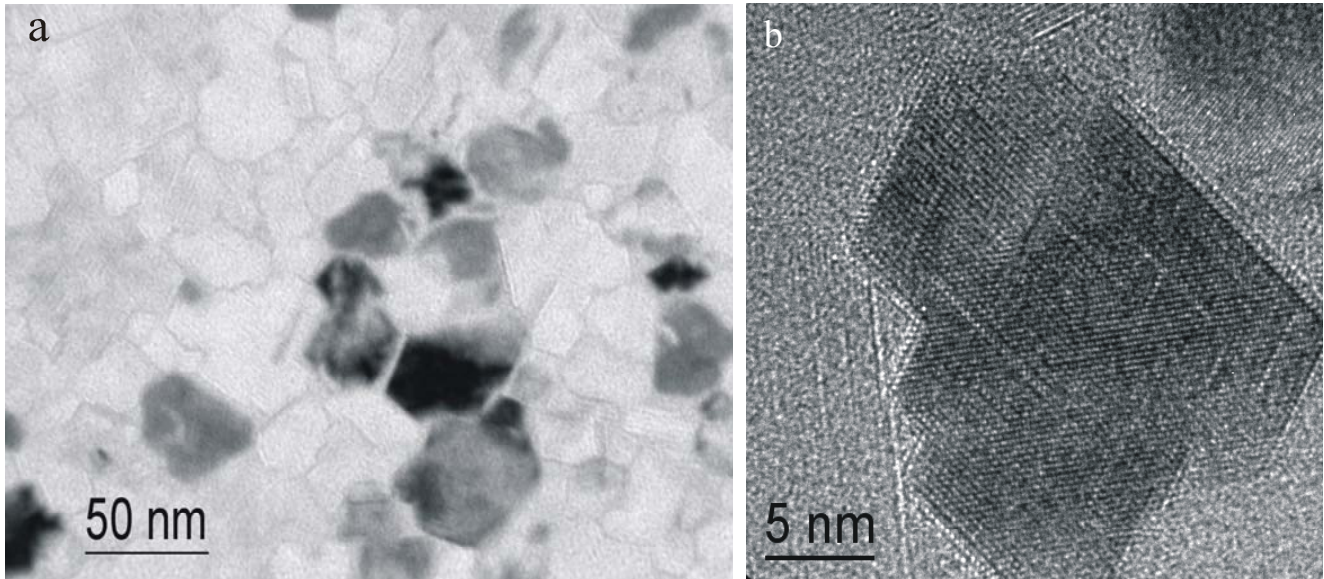


Fig.8 a. Bright-field TEM image showing the strong influence of the oxidation of a 10 nm thick $\text{Ge}_2\text{Sb}_2\text{Te}_5$ film resulting in crystallization at 35 instead of 130 °C and a totally different crystal morphology (cf. Fig.3). The deviating contrast of the grain boundaries indicate the presence of an amorphous phase, possibly GeO_x leading to a Ge depleted alloy with totally different crystallization behavior. **b.** HRTEM image showing a strongly faceted crystal surrounded by an amorphous phase.

It has been shown that the crystallization of $\text{Ge}_2\text{Sb}_2\text{Te}_5$ is nucleation driven (growth limited) [4]. On the other hand crystallization of Ag-In-Sb-Te [4] or doped eutectic Sb_2Te [18] is growth driven. The observation of large colonies at 130 °C in the present experiments on $\text{Ge}_2\text{Sb}_2\text{Te}_5$ seems to contradict that growth is the rate-limiting step. Several factors can explain the discrepancy. The experiments for proofing the nucleation-driven crystallization of $\text{Ge}_2\text{Sb}_2\text{Te}_5$ were performed in real disc structures, where the adjacent dielectric layers may have promoted nucleation. However, the same experiments and some others [16,19] indicated that the nucleation rate is reduced at the GeSbTe-ZnS/SiO_2 interface. So, this cannot be the explanation. On the other hand, it is likely that at 130 °C the amount of superheating is too small for a sufficient number of nuclei to form. In accordance with classical nucleation theory a slight increase in temperature results in an explosive increase in the number of stable nuclei. This increase is much stronger than the accompanying increase in growth rate. So, only in a small temperature interval, just above the critical temperature for crystallization large colonies can develop. Therefore in most experiments, using laser and thermal heating at higher temperatures (say from 150 °C and higher), with more superheating the large colonies will be absent. The present observation are not anomalous, because any phase transformation will show a temperature interval close to the one where the two phases are in equilibrium where the transformation is nucleation limited.

Typical bending-contour contrast of the spherulites as we observed with TEM (cf. Fig.3 and 4) was also observed, but not identified and recognized as such in the doped eutectic Sb_2Te phase change material [18]. Due to its growth-driven crystallization, this material will in general show this typical bending-contour contrast, whereas $\text{Ge}_2\text{Sb}_2\text{Te}_5$ will only show it just above the crystallization temperature.

The observation using the spherulites that crystal nucleation starts at the lowest temperature at the film/vacuum interface and not at the film/Si-nitride interface agrees well with the results obtained by [20] and by Ohshima [19] (T_c of a single $\text{Ge}_2\text{Sb}_2\text{Te}_5$ layer is 15 K lower than when this film is sandwiched between Si_3N_4 films). In fact, we did not really proof that nucleation occurs at the film/vacuum interface, but we showed that the bending within the colony is such that the center of

the spherulite is at the vacuum side. The most logical growth mode of a colony is that after nucleation, with a $\langle 111 \rangle$ axis perpendicular to the surface because of surface-energy minimization, the film starts to shrink locally and the surface becomes bended. Subsequent nucleation of neighboring grains is affected by the curved surface and by the orientation of the neighboring grains developed in the previous step. New grains will thus be slightly tilted with respect to the neighboring former ones. This growth mode explains the observed morphology with the correct type (sign) of the curvature.

Conclusions

The crystallization of amorphous $\text{Ge}_2\text{Sb}_2\text{Te}_5$ films (10, 40 and 70 nm thick) was studied by in-situ heating in a TEM. In a temperature interval between 70 and 125 °C crystallization only occurred when aided by the 200 kV electron beam. Using a 400 keV beam, crystallization was possible with the sample holder at room temperature. The reciprocal of the incubation time for crystallization turned out to scale linearly with the current density of the 400 keV beam. It was demonstrated that in principle the electron beam always affects the crystallization process. Nucleation is promoted by the electron beam and observations suggest that crystal growth is hampered. The main effect of the electron irradiation is displacement damage by knock-on collisions and not radiolysis or specimen heating.

At a temperature of 130 °C and higher crystallization also occurs without electron irradiation. Just above the critical temperature for crystallization large colonies (typical size 400 nm) of 10-20 nm crystallites develop showing typical high symmetry bending contour contrast. These colonies can be identified as thin top sections (a cap) of spherulites. They developed in the 40 and 70 nm thick films, but not in the 10 nm ones. Most abundant are spherulites with a $\langle 111 \rangle$ zone axis of the NaCl-type $\text{Ge}_2\text{Sb}_2\text{Te}_5$ structure perpendicular to the surface. Careful analysis shows that nucleation starts at the film/vacuum and not at the film/Si-nitride interface. At higher temperatures crystals in the spherulites coarsen and their mutual orientation relation is gradually lost and also voids develop in the film. At a temperature of 340 °C the transformation to the stable trigonal crystal structure (P 3 m1) of $\text{Ge}_2\text{Sb}_2\text{Te}_5$ occurs. The transition is characterized by very fast and excessive grain growth with the [0001] axis of the grains perpendicular to the surface. (Partial) oxidation of the $\text{Ge}_2\text{Sb}_2\text{Te}_5$ film resulted in a decrease of the crystallization temperature from 130 to 35 °C.

References

1. N. Yamada, E. Ohno, K. Nishiuchi, N. Akahira, *Jpn. J. Appl. Phys.* 26 (Suppl. 26-4, 1987), 61.
2. K. Nishimura, M. Suzuki, I. Morimoto, K. Mori, *Jpn. J. Appl. Phys.* 28 (Suppl. 28-3, 1989), 135.
3. H.J. Borg, R. van Woudenberg, *J. Magn. Magn. Mat.* 193 (1999), 519.
4. G.-F. Zhou, *Mat. Sci. Eng.* A304-306 (2001), 73.
5. T. J. Kono, R. Sinclair, *Mat. Sci. Eng.* A179/A180 (1994), 297; *ibid.*, *Acta Metall. Mater.* 42 (1994), 1231.
6. T. Nonaka, G. Ohbayashi, Y. Toriumi, Y. Mori, H. Hashimoto, *Thin Solid Films* 370 (2000), 258.
7. N. Yamada, T. Matsunaga, *J. Appl. Phys.* 88 (2000), 7020.
8. V. Weidenhof, I. Friedrich, S. Ziegler, M. Wuttig, *J. Appl. Phys.* 86 (1999), 5879.
9. B.J. Kooi, J.Th.M. De Hosson, *J. Appl. Phys.* 92 (2002), 3584; note that twice (in the caption of Fig.1 and in the Conclusions) erroneously the value 1.827 nm is given for the c lattice constant instead of the correct value 1.727 nm.
10. A.K. Petford-Long, R.C. Doole, C.N. Alfonso, J. Solis, *J. Appl. Phys.* 77 (1995), 607.
11. J. Vrijmoeth, H.A. van der Vegt, J.A. Meyer, E. Vlieg, R.J. Behm, *Phys. Rev. Lett.* 72 (1994), 3843; H.A. van der Vegt et al., *Surf. Sci.* 365 (1996), 205; H.A. van der Vegt et al., *Phys. Rev. B* 57 (1998), 4127.
12. M. Chen, K.A. Rubin, R.W. Barton, *Appl. Phys. Lett.* 49 (1986), 502.
13. E. Morales-Sanchez, E. Prokhorov, Yu. Vorobiev, J. Gonzalez-Hernandez, *Solid State Commun.* 122 (2002), 185.
14. M.H.R. Lankhorst, *J. Non-Cryst. Solids* 297 (2002), 210.
15. I. Friedrich, V. Weidenhof, S. Lenk, M. Wuttig, *Thin Solid Films* (2001), 239.
16. G. Ruitenber, A.K. Petford-Long, R.C. Doole, *J. Appl. Phys.* 92 (2002), 3116.
17. D. B. Williams, C.B. Carter, *Transmission Electron Microscopy Vol.1*, pp 61-65, Plenum Press, New York, 1996.
18. H. Borg, M. Lankhorst, E. Meinders, W. Leibrandt, *Mat. Res. Soc. Symp. Proc.* 674 (2001), V1.2.1; H.J. Borg, M. van Schijndel, J.C.N. Rijpers, M.H.R. Lankhorst, G. Zhou, M.J. Dekker, I.P.D. Ubbens, M. Kuijper, *Jap. J. Appl. Phys.* 40 (2001), 1592.
19. N. Ohshima, *J. Appl. Phys.* 79 (1996), 8357.
20. T.H. Jeong, M.R. Kim, H. Seo, S.J. Kim, S.Y. Kim, *J. Appl. Phys.* 86 (1999), 774.